Characterization of spatial heterogeneity in groundwater applications

PhD Thesis

Department of Geotechnical Engineering and Geo-Sciences (ETCG)

Technical University of Catalonia, UPC

Paolo Trinchero

February 2009

HYDROGEOLOGY GROUP
TECHNICAL UNIVERSITY OF CATALONIA

Chapter 5

Influence of Heterogeneity on the Interpretation of Pumping Test Data in Leaky Aquifers *

5.1 Introduction

In this paper, we simulate pumping tests in synthetically generated aquifer-aquitard systems, considering separately the heterogeneity of the pumping aquifer and the confining aquitard. Estimates of the apparent hydraulic parameters are obtained by analyzing each pumping test independently for different distances from the pumping well and using common methods available in the literature and used extensively in computer codes developed for the analysis of pumping tests. By combining the estimates of the apparent parameters obtained with the different analysis methods, it is shown that information about the heterogeneity of the system may be inferred.

*This chapter is based on the article: Copty, N. K., P. Trinchero, X. Sanchez-Vila, M. Sarioglu, and A. Findikakis (2008 accepted for pubblication)), Influence of heterogeneity on the interpretation of pumping test data in semiconfined aquifers, *Water Resources Research*.

It is important to note that the interpretation of pumping tests conducted in heterogeneous media can, in principle, be formulated as a geostatistical or inverse problem. Over the past two decades several inversion modeling tools have been developed (see for example [79]). Some authors have also proposed the use of hydrological tomography for the estimation of spatial distribution of the flow parameters ([102]; [104]) However, the computational effort involved in these interpretation approaches can be intensive and quite complex due to the ill-posedness of the groundwater inverse problem. The goal in this paper is to explore the possibility of extending commonly used pumping tests analysis procedures to extract information about the underlying spatial variability of leaky aquifer systems.

5.2 Problem Statement

The system considered in the development of this methodology is the same as that defined by *Hantush and Jacob* [44] and described in section 4.1.

5.2.1 Existing Parameter Interpretation Methods

Two procedures are commonly used in the analysis of time-drawdown data in leaky aquifers: (1) the inflection-point method [42], and (2) the curve fitting method [99]. Both methods are based on the assumption of homogeneity of the system, plus a number of additional somewhat restrictive assumptions, such as no storage released from the aquitard and constant head in the unpumped aquifer. Subsequent to the original study by *Hantush and Jacob* [44], a number of papers relaxed some of the assumptions listed above. For example, *Hantush* [45] accounted for the storage of the confining layer. [68, 69] provided a more general solution including drawdown in the overlying aquifer. *Moench* [63] incorporated the effect of the extraction well diameter and well bore skin on the transient drawdown of leaky aquifers. Despite these improvements, the above-mentioned methods remain quite popular for the interpretation of pumping test data in leaky aquifers due to

their relative simplicity.

A more detailed description of both the inflection-point method and the curve fitting method is provided in section 4.3.

In this paper, the best-fit parameters were determined by a trial and error approach that minimizes the sum of squared differences between the simulated drawdown and the theoretical drawdown:

$$\sum_i [\overline{s}(r, t_i) - s(r, t_i)]^2 \tag{5.1}$$

where $\overline{s}(r, t_i)$ is the observed drawdown at distance r from the pumping well and time t_i and $s(r, t_i)$ is the theoretical drawdown derived from the type curves.

Recently, a third method for the interpretation of pumping tests in leaky aquifers was developed, referred to as the double inflection-point (DIP) method [93]. A detailed description of the DIP method is provided in chapter 4.4.1.

The above methods provide the exact solution for the hydraulic parameters (T, S, B) in a homogenous system, provided the drawdown data are noise-free. On the other hand, each method provides a different set of parameters in real (heterogeneous) systems, since each particular method gives more weight to different portions of the time-drawdown data. The emphasis that each method gives to the different portions of the drawdown curve is discussed further in *Trinchero et al.* [93] and in Section 5.3.3 of this paper. One of the main conclusions of *Trinchero et al.* [93] was that by comparing the estimates of provided by the inflection-point method [42] and the DIP method, it is possible to infer information about the local transmissivity in the vicinity of the pumping well.

In this study Monte Carlo simulations are used to assess what parameter values are given by the different methods and whether it is possible to relate these parameters to some characteristic values of the heterogeneous system.

5.2.2 Numerical Setup

We model the natural logarithms of the transmissivity and aquitard hydraulic conductance as two independent multivariate Gaussian SRF's with stationary exponential semivariograms. Two sets of simulations are presented. In the first one the transmissivity of the pumped aquifer was assumed spatially variable while the aquitard conductance is assumed uniform. In the second set, the aquifer was assumed to be homogeneous and the aquitard heterogeneous. This allows us to evaluate the impact of the heterogeneity of the aquifer and the confining layer on the estimated parameters independently. For each set of parameters, 1000 realizations of the spatially variable parameter (aquifer transmissivity or aquitard conductance) were generated using the turning bands method [60]. The storativity of the pumped aquifer was assumed to be uniform equal to 0.0001. The confining aquifer was assumed to have no storage, which is consistent with the leaky aquifer system analyzed by [44]. The pumping well is located at the centre of a square aquifer, 481 m on each side. The medium was discretized using square cells of size 1 x 1 m^2. At steady state, the equivalent well radius is approximately 0.2 times the cell size (Desbarats, 1992). A prescribed head condition was imposed at the outer boundary, and the extraction well is treated as a prescribed sink term with steady rate of 2 m^3/day. Drawdowns were simulated using the finite difference model MODFLOW [46]. The test duration was 2 days, and a variable time step was used in the simulations, starting with 1 s, and gradually increasing it as the test progressed.

Inspection of the results showed that steady state was reached at the end of the 2-day period for all cases considered. Some simulations were repeated with a no-flow condition at the outer boundary and the simulated drawdown data were identical, indicating that the outer boundary had no impact on the simulated drawdowns. The numerical setup was also tested by simulating the pumping test in a homogeneous leaky aquifer system and comparing the drawdown data to Equation 4.6.

5.3 Results

5.3.1 Impact of Aquifer Heterogeneity

The first set of results corresponds to the case with spatially uniform aquitard conductance ($Co = 0.001 day^{-1}$) and spatially variable aquifer transmissivity (with geometric mean, $Tg = 1m2/day$, and integral scale: $I = 8m$, and variance: $\sigma^2 = 1$). Figure 5.1 compares the aquifer transmissivity estimates (normalized by T_g) using the inflection-point and the curve-fitting methods at different distances from the pumping well. Each point on the plots corresponds to one of the 1000 Monte Carlo realizations. Figure 5.1 also shows the correlation ($Corr$) and the mean absolute difference (MAD) between the two sets of estimates as a function of distance. From the two options of the inflection-point method described in Section 4.4, we selected to use the slope and drawdown at the point corresponding to half the steady state drawdown.

From Figure 5.1 we observe that overall the transmissivity estimates obtained with the two methods tend to spread around the 1:1 line. The differences between the values estimated with the two methods come from each model weighing differently the T values within the domain. For larger distances from the pumping well, the estimates with the two methods tend to converge, since the larger aquifer volume involved in the weighting process averages out the effect of heterogeneities. The convergence in the estimates is also reflected in the increasing $Corr$ towards 1 and decreasing MAD towards zero with distance.

There is a significant difference between the behavior of leaky and confined aquifers during pumping tests. In the latter, it was shown analytically by *Sanchez-Vila et al.* [83] that eventually all the estimated transmissivity values converge to a single T value which is close to the geometric average of the random function $T(x, y)$. On the other hand, for pumping tests conducted in leaky aquifers, each realization yields potentially different estimates. The reason is that in confined aquifers steady state conditions are never reached, and so, all points in the domain are eventually

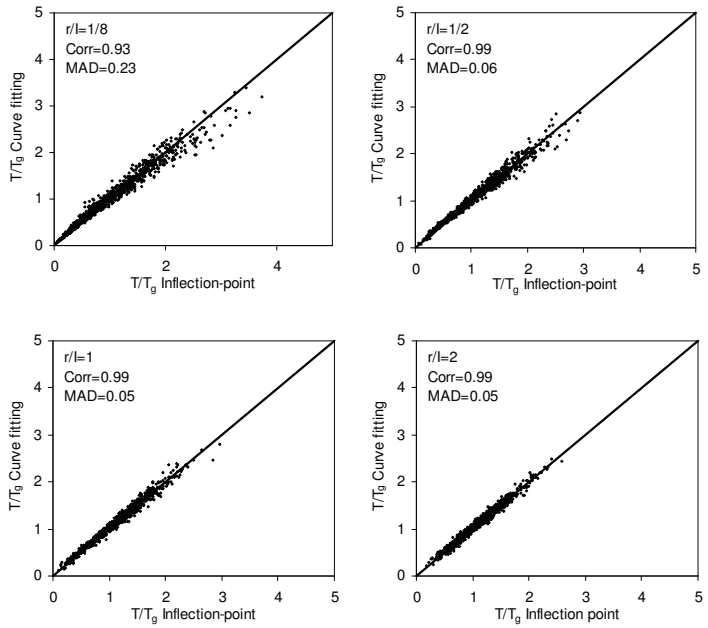

Figure 5.1: Normalized transmissivity estimates using the inflection-point and the curve fitting methods for different distances from the pumping well (heterogeneous aquifer with geometric mean, $Tg = 1m^2/day$, $\ln T$ integral scale $I = 8m$, $\sigma^2 = 1$, and a uniform aquitard with $Co = 0.001day^{-1}$).

affected by pumping. This is not the case in leaky aquifers, where steady state conditions are eventually reached, and the drawdown is null everywhere except within a (limited) volume around the pumping well. Thus, the weighted average of the local T values can be different for each individual realization and, in particular, different from the overall mean value, T_g. Figure 5.2 displays scatter plots of the normalized aquitard conductance estimates from both the inflection-point and the curve fitting methods. For small distances from the pumping well, the estimates with the two methods may differ significantly and the scatter of the estimated aquitard conductance values is greater than the scatter of the aquifer transmissivity values. For large distances the estimates become independent of the interpretation method. However, for many simulations the estimated values can be significantly different from the actual value used in the drawdown simulation (i.e., $C/C_0 \neq 1$). These observations are also confirmed by the values of $Corr$ and MAD which ap-

proach one and zero, respectively with increase in distance. A similar behavior is observed for the estimated storativity (The results are not presented here for brevity).

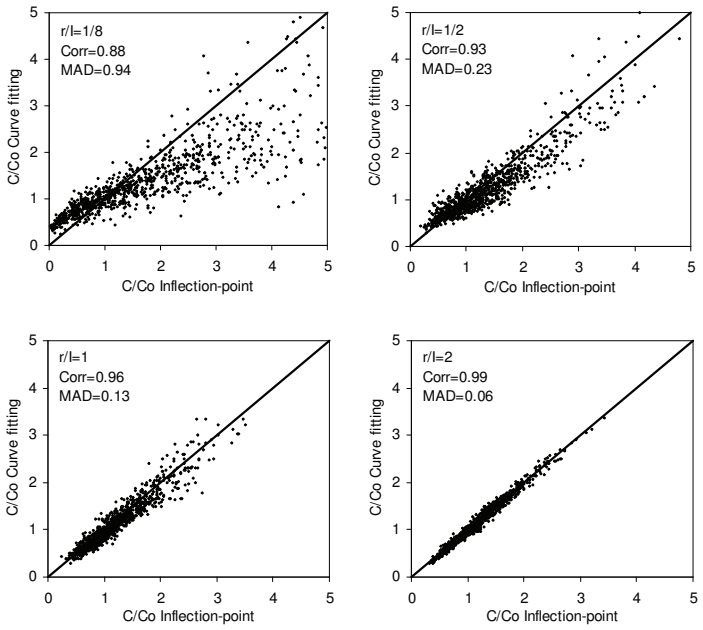

Figure 5.2: Normalized aquitard conductance estimated using the inflection-point and the curve fitting methods for different distances from the pumping well (heterogeneous aquifer with $T_g = 1m2day^{-1}$, $I = 8m$, and $\sigma^2 = 1$, and a uniform aquitard with $Co = 0.001day^{-1}$).

The main low-order statistics of the flow parameters estimates are compiled in Table 5.1. The mean of the T estimates is found to be between the geometric and arithmetic mean of the transmissivity (in this case $T_a/T_g = 1.65$). *Copty et al.* [18] observed a similar behavior in the equivalent transmissivity for steady state radially convergent flow in leaky aquifers and associated this effect to each realization sampling only a portion of the domain centered around the pumping well, thus forcing the expected mean towards the arithmetic average. Table 5.1 also shows a slight increasing trend in the mean of estimated transmissivity with distance. This observation is discussed later.

The deviation of the estimated T values from the actual distributions causes a bias in the

Table 5.1: Expected value and standard deviation (shown in parenthesis) of the flow parameters function of distance from the well- Case of spatially variable aquifer.

Parameter	Interpetation Method	Distance from the Well r/I					
		1/8	1/2	1	2	4	8
Normalized Transmissivity	Inflection-point	1.06 (0.66)	1.07 (0.58)	1.07 (0.46)	1.07 (0.38)	1.11 (0.32)	1.24 (0.32)
	Curve fitting	1.07 (0.61)	1.08 (0.52)	1.08 (0.45)	1.08 (0.38)	1.12 (0.32)	1.24 (0.32)
Normalized Leakage Factor	Inflection-point	1.03 (1.01)	1.01 (0.49)	1.01 (0.40)	1.03 (0.33)	1.06 (0.26)	1.09 (0.19)
	Curve fitting	0.93 (0.49)	1.03 (0.43)	1.05 (0.40)	1.06 (0.35)	1.07 (0.27)	1.09 (0.20)
Normalized Conductance	Inflection-point	2.48 (2.76)	1.34 (0.76)	1.20 (0.54)	1.13 (0.48)	1.07 (0.39)	1.08 (0.30)
	Curve fitting	1.74 (1.64)	1.22 (0.66)	1.15 (0.53)	1.11 (0.49)	1.08 (0.39)	1.08 (0.29)
Normalized Storativity	Inflection-point	1.98 (2.88)	1.25 (0.47)	1.19 (0.37)	1.16 (0.42)	1.14 (0.39)	1.19 (0.34)
	Curve fitting	1.61 (1.68)	1.18 (0.33)	1.17 (0.37)	1.16 (0.42)	1.14 (0.39)	1.18 (0.33)

storativity and aquitard conductance estimates, which in the mean are slightly overestimated. The reason comes from the interpretation methods, all of them leading to estimates that are not independent, but correlated. Thus, errors in the estimation of one parameter directly translate to errors in the remaining parameters. All methods have a large uncertainty, as measured by the standard deviation (Table 5.1). For large distances the variances decrease and the estimates become more consistent.

The probability density function (pdf) of the T/Tg estimates from the inflection-point method (depicted in Figure 5.1) is shown in Figure 5.3. The pdf of T/T_g is shown for different r/I values. For comparison, the (lognormal) distribution of the transmissivity values used in the generation of the heterogeneous T field is also shown. It is observed that all distributions are asymmetric with positive skewness. For observation points very close to the pumping well, the pdf of T/T_g is close to the log-normal distribution of the transmissivity field used in the pumping test simulation. As the value of r/I increases, the variance of T/T_g decreases. However, even for large values of r/I,

the variance of T/T_g does not approach zero and, hence, the estimated transmissivity may differ from the geometric mean. As noted above, this is a significant difference in the behavior of leaky and confined aquifers where, in the latter case, the cone of depression continues to grow with time and a much larger aquifer volume contributes flow towards the pumping well.

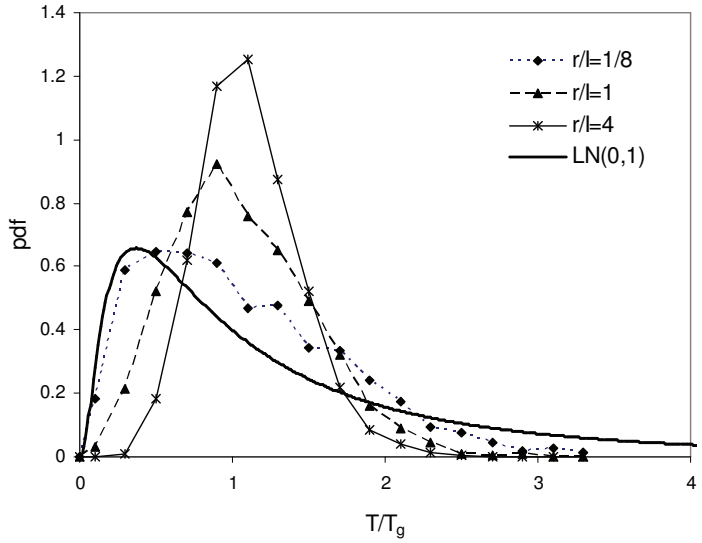

Figure 5.3: Probability density function of T/Tg estimated using the inflection-point method at different distances from the well. The lognormal $LN(0,1)$ distribution is also shown. (heterogeneous aquifer with $T_g = 1m2day^{-1}$, $I = 8m$, and $\sigma^2 = 1$, and a uniform aquitard with $Co = 0.001day^{-1}$).

The distribution of the T/T_g estimates is dependent on the parameters of the aquifer-aquitard system, namely the values of C, I, and the σ^2. Figure 5.4 presents the pdf value of the T/T_g estimates for different sets of parameters and for $r/I = 1$. With increase in the σ^2, the variability of the transmissivity field increases and consequently, the pdf of the estimated T displays larger variance and skewness. As I or C increases, the aquifer radius perturbed by the pumping test relative to the characteristic length of the transmissivity distribution diminishes. This yields estimates that are influenced more by the transmissivity near the pumping well and, hence, the pdf becomes closer to the log-normal distribution used in the generation of the T field.

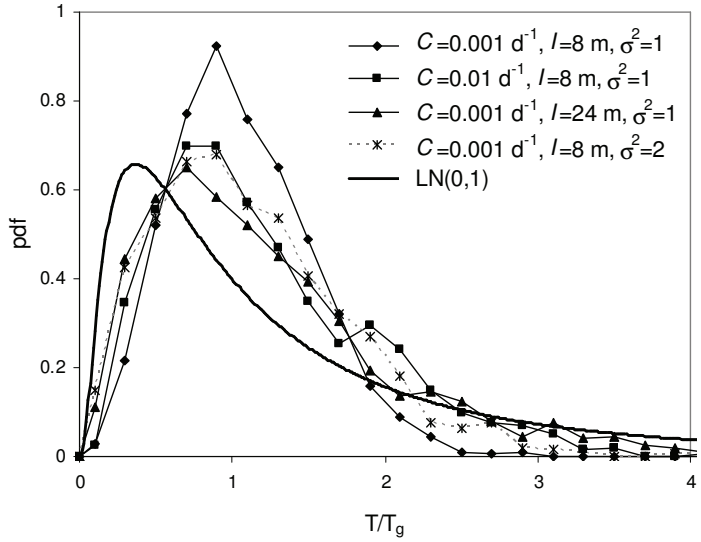

Figure 5.4: Sensitivity of the T/T_g pdf estimated using the inflection-point method to the conductance and log-transmissivity integral scale and variance. The lognormal distribution $LN(0, 1)$ is also shown.

5.3.2 Spatial Variability of the Estimated Flow Parameters

Figure 5.5 (a,b) shows the estimates of leakage factor and transmissivity (normalized by $B_g = (T_g/C_o)^{1/2}$ and T_g respectively), for selected simulations and as a function of distance of the observation well from the pumping well. Only the estimates which were obtained with the inflection-point method are shown (those with the curve fitting method are qualitatively similar). The resulting estimates are strongly dependent on the distance of the observation point from the pumping well and even for large distances ($r/I = 8$) generally display a noticeable variation for every individual realization. This behavior is very different to the confined case, where for large distances all the values of estimated transmissivities tend to converge to a single value that is close to the geometric mean of the T field [62, 83].

These results can potentially have significant implications in real applications where flow parameters estimated from pumping tests are used in geostatistical studies and for defining input

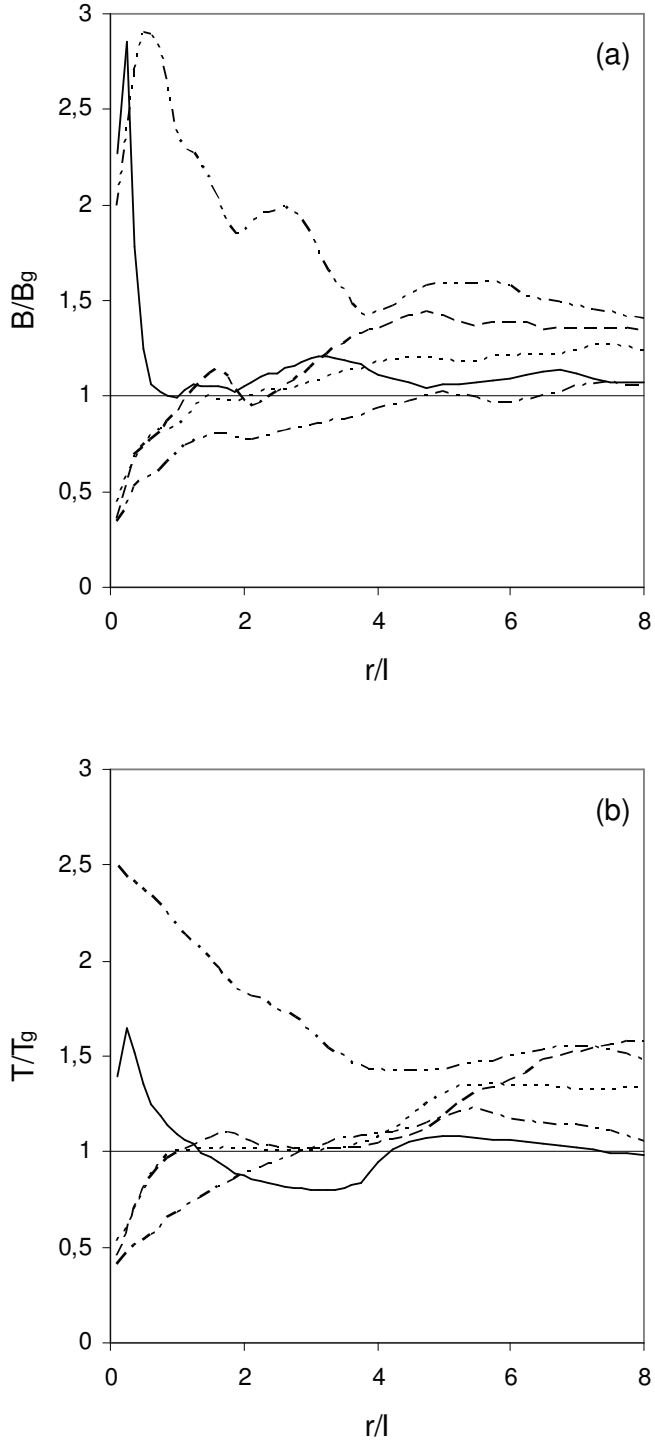

Figure 5.5: (a) Leakage factor normalized by $B_g = (T_g/C_o)^{1/2}$ and (b) transmissivity normalized by T_g estimated using the inflection-point method for randomly selected simulations as a function of distance from the well.

parameters of groundwater flow models. Specifically, pumping tests conducted in the same formation would yield different flow parameters depending on the leakage into the pumped aquifer and on the location of the observation point relative to the pumping well.

The spatial variability of the flow parameters is also observed in the ensemble mean of the flow parameters, average over the 1000 Monte Carlo simulations. Figure 5.6(a,b) shows a comparison of the mean estimates of the leakage factor and transmissivity obtained from the different interpretation methods as a function of distance. Close to the pumping well, the mean leakage factors obtained with the different interpretation methods show large variations. With increasing distance, the mean estimates converge to a value slightly larger than the geometric mean, B_g . This effect can be explained by physical considerations. For heterogeneous leaky aquifers, the steady state drawdown can be expressed as an extension of Equation 4.4:

$$s_m = \frac{Q}{2\pi T_m} K_0(r/B_m) \tag{5.2}$$

where s_m is the steady state drawdown and T_m and B_m are the apparent transmissivity and leakage factor, respectively, at steady state. Similarly, the drawdown derivative at the inflection-point can be expressed using the *Hantush* [42] analytical solution as:

$$\Delta s_p = \frac{2.3Q}{4\pi T_p} \exp(-r/B_p) \tag{5.3}$$

where Δs_p is the slope of the drawdown curve at the inflection-point and T_p and B_p are the apparent transmissivity and leakage factor, respectively, at the inflection point. Taking the ratio of Equations 5.2 and 5.3 yields a somewhat modified version of Equation 4.2:

$$2.3\frac{s_m/2}{\Delta s_p} = \frac{T_p}{T_m} \exp(r/B_p) K_0(r/B_m) \tag{5.4}$$

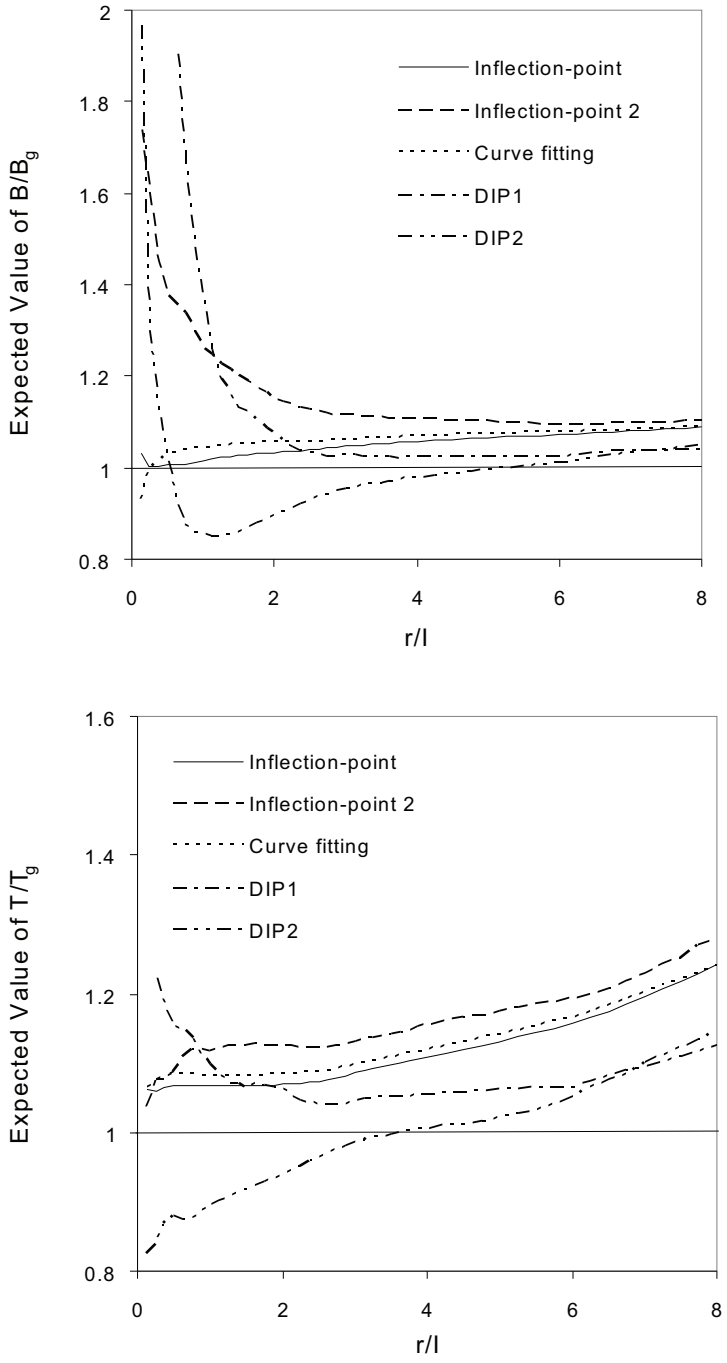

Figure 5.6: Expected value of the (a) Leakage factor normalized by $B_g = (T_g/C_o)^{1/2}$ and (b) transmissivity normalized by T_g as a function of distance from the well (heterogeneous aquifer with $T_g = 1m2day^{-1}$, $I = 8m$, and $\sigma^2 = 1$, and a uniform aquitard with $Co = 0.001day^{-1}$).

Whereas T_m and B_m result from drawdown data at late times and, hence, are influenced by a larger aquifer volume, T_p and B_p are estimated from data at much earlier times. For observation points located close to the well, T_p and B_p may significantly differ from T_m and B_m. As the distance from the pumping well increases, the drawdown curve involves a larger portion of the aquifer, with the ratios T_p/T_m and B_p/B_m moving progressively closer to one. Both ratios however do not necessarily converge to 1 because of the limited aquifer volume that influences pumping tests in leaky aquifer. Thus, for large distances the response of the heterogeneous system approaches somewhat that of an equivalent homogeneous system. A similar analysis could also be applied to the DIP method since it also combines observations of the drawdown curve and its derivatives at different times.

Figure 5.6 also shows the expected value of the normalized B and T estimates corresponding to the two variants of the inflection-point method, namely (1) from the slope at the point corresponding to half the steady state drawdown (denoted as Inflection-Point in the figure), and (2) from the maximum slope of the drawdown curve (Inflection-Point 2 in the figure). In the latter case, the corresponding expression relating the ratio of drawdown to drawdown slope at the inflection-point to the leakage factor is:

$$2.3\frac{s_p}{\Delta s_p} = \exp(r/B_p)K_0(r/B_p) \tag{5.5}$$

As evidenced by Equation 5.4, the leakage factor estimated with the first variant of the inflection-point method actually depends on the apparent parameters at both intermediate and late (steady) time. On the other hand, from Equation 5.5 we see that estimates obtained with the Inflection-Point 2 are influenced by the apparent hydraulic parameters at intermediate times only. Hence, the former interpretation (Equation 5.4) of the inflection-point method is relatively less dependent on the local conditions around the pumping well than Inflection-Point 2.

Another point observed in Figure 5.6 is the increasing trend in both the estimated leakage

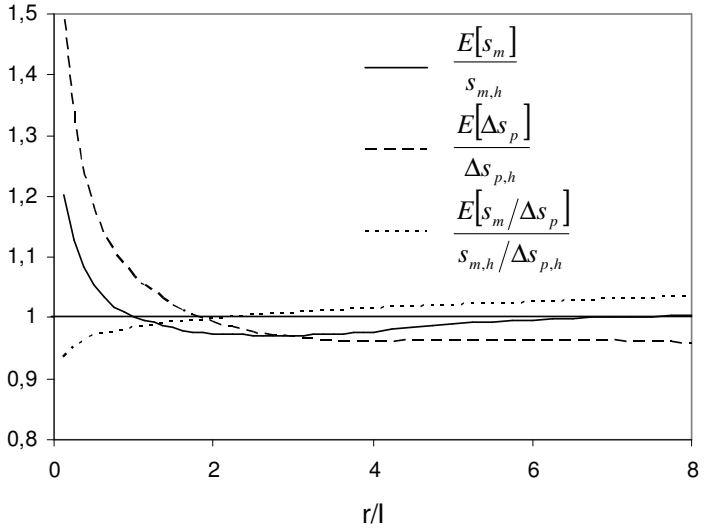

Figure 5.7: Comparison of the mean steady state drawdown and drawdown slope at the inflection-point for a case of spatially variable transmissivity to that of the homogeneous aquifer with transmissivity T_g.

factor and transmissivity with distance obtained regardless of the interpretation method (except for low values of r/I). The explanation behind this trend for the inflection-point method is as follows. Figure 5.7 shows the expected values of s_m, Δs_p, and $s_m/\Delta s_p$. All three quantities are normalized by their counterparts $s_{m,h}$, $\Delta s_{p,h}$, and $s_{m,h}/\Delta s_{p,h}$ corresponding to the homogeneous aquifer with transmissivity equal to T_g. For large distances both s_m and Δs_p are underestimated, but s_m converges faster to its homogeneous counterpart, so that the normalized ratio $s_m/\Delta s_p$ is greater than 1 and increases monotonously in the range of distances explored. From Equation 4.2, the direct consequence of overestimating $s_m/\Delta s_p$ is to underestimate B, and, subsequently, underestimate T (Figure 5.6b).

A similar increasing trend in the estimated transmissivity of the pumped aquifer with distance between the observation and pumping wells was also observed by *Neuman and Witherspoon* [69]. Their analysis however was for the case of homogeneous media, with the apparent increase in the estimated transmissivity with distance resulting when the storage of the aquitard is neglected. As

noted above, the apparent increase in our case is due to the heterogeneity of the aquifer and the fact that data from different times are used in the data interpretation.

5.3.3 Identification of the Local Transmissivity at the Pumping Well

As indicated by *Trinchero et al.* [93], the DIP method can potentially be used to infer additional information on the local contrast of the transmissivity in the vicinity of the pumping well relative to the transmissivity spatial mean. To illustrate this, the DIP method and inflection-point method are jointly applied to the Monte Carlo simulations. Figures 5.8 and 5.9 compare the transmissivity estimates obtained from the inflection-point method with the two estimates obtained from the DIP method (DIP1 and DIP2), respectively, for two different distances from the pumping well ($r/I = 1/2$ and $r/I = 2$).

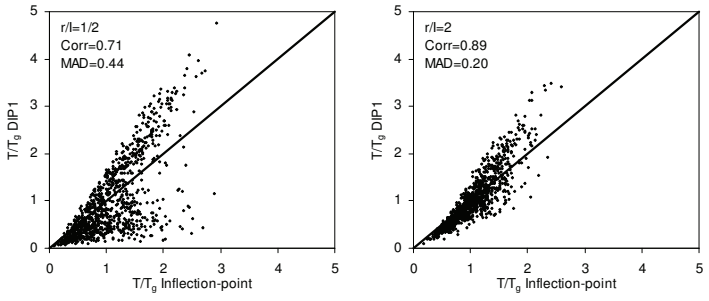

Figure 5.8: Normalized transmissivity estimated using the inflection-point and the DIP1 (positive peak) methods for $r/I = 1/2$ and $r/I = 2$ (heterogeneous aquifer with $T_g = 1m2day^{-1}$, $I = 8m$, and $\sigma^2 = 1$, and a uniform aquitard with $Co = 0.001day^{-1}$).

Although the agreement among the different estimates improves with increase in distance from the pumping well, large differences are observed for some realizations. This is a result of each method giving emphasis to different portions of the time-drawdown data. The DIP1 method uses early time drawdown data, and thus it tends to provide estimates that are representative of a very small volume around the pumping well. Therefore, it tends to yield T estimates closer to the transmissivity near the pumping well. On the other hand, the DIP2 method places more emphasis on

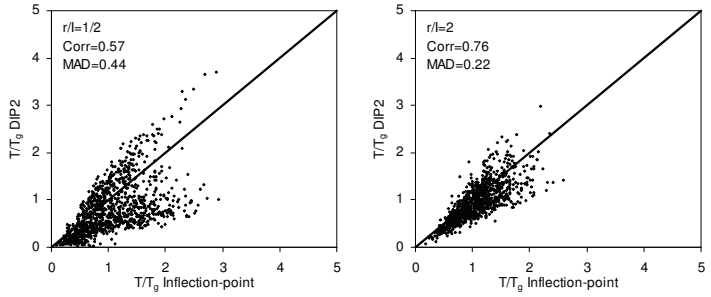

Figure 5.9: Normalized transmissivity estimated using the inflection-point and the DIP2 (negative peak) method for r/I=1/2 and r/I=2 (heterogeneous aquifer with $T_g = 1m2day^{-1}$, $I = 8m$, and $\sigma^2 = 1$, and a uniform aquitard with $Co = 0.001day^{-1}$).

the late portion of the drawdown, providing T values that are representative of large aquifer volumes. As a consequence, the geometric average of the estimates from the two DIP methods which is presented in Figure 5.10 agrees better with the inflection-point estimates than each method individually. This can also be seen in the values of *Corr* and *MAD* shown on Figures 5.8-5.10.

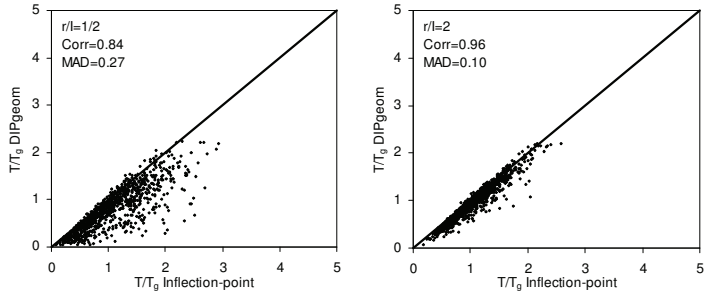

Figure 5.10: Normalized transmissivity estimated using the inflection-point method and the geometric mean of the two DIP estimates for $r/I = 1/2$ and $r/I = 2$ (heterogeneous aquifer with $T_g = 1m2day^{-1}$, $I = 8m$, and $\sigma^2 = 1$, and a uniform aquitard with $Co = 0.001day^{-1}$).

From the estimates obtained with the inflection-point (Hantush), DIP1 and DIP2 methods it is possible to infer information about the local transmissivity at the pumping well. For this purpose three correlation functions are defined:

- $C(T_w, T_{D1} - T_H)$ is a measure of the correlation of the transmissivity at the pumping well to

the difference between the inflection-point and DIP1 estimates

- $C(T_w, T_H - T_{D2})$ is a measure of the correlation of the transmissivity at the pumping well to the difference between the inflection-point and DIP2 estimates

- $C(T_w, T_{D1} - T_{D2})$ is a measure of the correlation of the transmissivity at the pumping well to the difference between the DIP1 and DIP2 estimates.

The correlation coefficients were computed using the parameter values estimated from the time-drawdown data of individual simulations for different distances from the pumping well, and then by averaging over the 1000 Monte Carlo simulations. Because the estimates T_{D1}, T_H, and T_{D2} are influenced by progressively larger aquifer volumes, positive values of the three correlations $T_{D1}-T_H$, T_H-T_{D2} or $T_{D1}-T_{D2}$ with T_w are indicative of a local T_w larger than the aquifer T spatial mean and vice versa. The three correlation functions are shown in Figure 5.11 as a function of distance from the pumping well. The correlation functions tend to vanish with distance, indicating that far from the well all the estimates are independent of the local T value at the pumping well. On the other hand, observation points located at $r < I$ would provide the greatest information about the local transmissivity.

Finally, we note that from previously published work (e.g., *Desbarats* [25], *Copty et al.* [18]), one would expect that the representative local transmissivity would be a time-dependent weighted average of the point T values surrounding the pumping well, with weights decreasing with distance. Since the correlations displayed in Figure 5.11 are in terms of the single transmissivity value at the pumping well, T_w, only partial correlations are observed.

5.3.4 Impact of Aquitard Heterogeneity

In this section we consider the scenario where the aquifer is assumed to be homogeneous with transmissivity $T_o = 1m^2/day$, while the aquitard conductance is assumed to be a multi-logGaussian

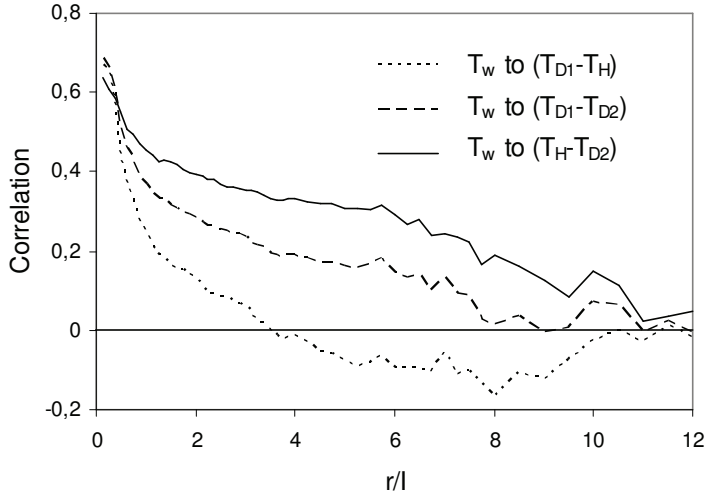

Figure 5.11: Correlation of the difference in the estimated transmissivity values obtained from different methods to the transmissivity at the well (heterogeneous aquifer with $T_g = 1m2day^{-1}$, $I = 8m$, and $\sigma^2 = 1$, and a uniform aquitard with $Co = 0.001day^{-1}$).

SRF with a geometric mean $C_g = 0.001day^{-1}$. The variance and integral scale of the natural log transform of the conductance, $\ln C$, are 1 and 8 m, respectively. For comparison purposes, these are identical to what was used earlier for the case of homogeneous aquitard and spatially variable transmissivity.

The normalized transmissivity and conductance estimates obtained from the inflection-point and the curve fitting methods for different distances from the pumping well are presented in Figures 5.12 and 5.13, respectively. The values used for normalization are: T_o and $C_g = 0.001day^{-1}$. Table 5.2 provides the expected values and standard deviations of all the estimated flow parameters, including storativity and leakage factor, at different distances.

In this scenario, both estimation methods yield very similar transmissivity and storativity estimates, as seen also in the values of $Corr$ and MAD. Further, for short distances, normalized expected values of T and S are very close to 1 with a very small standard deviation (Table 5.2). For larger distances, although the estimates obtained with both methods are in good agreement

Table 5.2: Expected value and standard deviation (shown in parenthesis) of the flow parameters function of distance from the well- Case of spatially variable aquitard.

Parameter	Interpetation Method	Distance from the Well r/I					
		1/8	1/2	1	2	4	8
Normalized Transmissivity	Inflection-point	0.98 (0.01)	1.00 (0.05)	1.01 (0.08)	1.04 (0.15)	1.13 (0.27)	1.39 (0.44)
	Curve fitting	0.98 (0.03)	1.00 (0.06)	1.02 (0.09)	1.05 (0.16)	1.13 (0.26)	1.34 (0.36)
Normalized Leakage Factor	Inflection-point	0.82 (0.15)	0.82 (0.13)	0.82 (0.11)	0.84 (0.10)	0.86 (0.08)	0.89 (0.06)
	Curve fitting	0.81 (0.13)	0.83 (0.12)	0.83 (0.11)	0.84 (0.09)	0.86 (0.08)	0.89 (0.06)
Normalized Conductance	Inflection-point	1.63 (0.74)	1.61 (0.61)	1.59 (0.54)	1.56 (0.50)	1.58 (0.52)	1.78 (0.67)
	Curve fitting	1.65 (0.65)	1.57 (0.55)	1.56 (0.52)	1.55 (0.49)	1.59 (0.53)	1.76 (0.63)
Normalized Storativity	Inflection-point	0.97 (0.01)	1.00 (0.02)	1.01 (0.02)	1.02 (0.07)	1.07 (0.17)	1.27 (0.33)
	Curve fitting	0.99 (0.02)	1.00 (0.02)	1.01 (0.03)	1.02 (0.08)	1.08 (0.17)	1.25 (0.28)

with each other, they deviate in many instances from To (see Table 5.2 and Figure 5.12). This indicates that, as the distance between the observation point and pumping well increases, the spatial variability of the aquitard conductance is expected to have a larger influence on the estimation of the transmissivity.

The expected value of the estimated conductance on the other hand is close to the arithmetic mean ($C_g \exp(\sigma^2/2) = 1.65 \cdot 10^{-3} day^{-1}$), which translates into a mean estimated leakage factor smaller than the geometric mean defined as $L_g = (T_0/C_g)^{1/2}$. The standard deviation tends to slightly decrease with distance (Table 5.2 and Figure 5.13).

This behavior can be explained by looking at the vertical fluxes through the semiconfining layer of a homogeneous leaky aquifer system. We consider an observation well at distance r_{obs} from the pumping well. The time corresponding to the inflection point for this observation well is given by: $t_p = r_{obs} S B/2T$. At this moment in time (time of inflection), the leaky well function at any distance r from the pumping well is $W(u, r/B)$ where $u = \frac{r^2 S}{4 t_p T} = \frac{(r/B)^2}{2 r_{obs}/B}$. A plot of $W(u, r/B)$

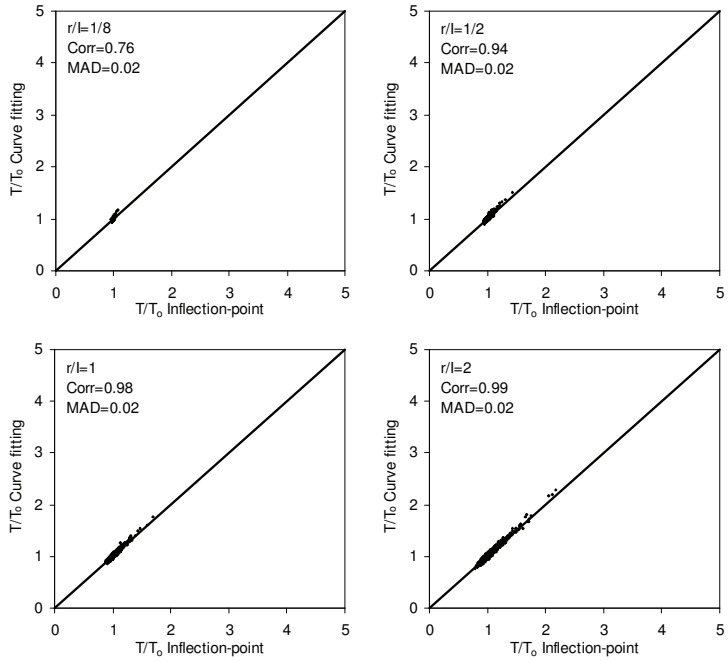

Figure 5.12: Normalized transmissivity estimated using the inflection-point and the curve fitting methods for different distances from the pumping well (uniform aquifer with $T_o = 1m^2/day$, and spatially variable aquitard with $C_g = 0.01day^{-1}$, $I = 8m$, and $\sigma^2 = 1$)

as a function r/B at $t_p = r_{obs}SB/2T$ and for different values of r_{obs}/B is shown in Figure 15a. Integrating the leaky well function over the entire aquifer yields the ratio of the cumulative vertical flow though the aquitard to the pumping rate at the well, which is shown in Figure 15b. For small values of robs/B, only a small fraction of the pumped water is leakage through the confining layer. As such, the pumping test is influenced by the local aquitard conductance only. That is, the pumping test is not influenced by the spatial variability of the aquitard conductance, explaining why at short distances the expected value of the estimated transmissivity shows no spread around its actual value (Figure 13a). As r_{obs}/B increases, the perturbed confining layer volume increases and the vertical flow constitutes a larger fraction of the pumping rate. For such conditions, the pumping test would yield a weighted spatial average of the aquitard conductance and as a result, the transmissivity estimate would deviate from the actual values.

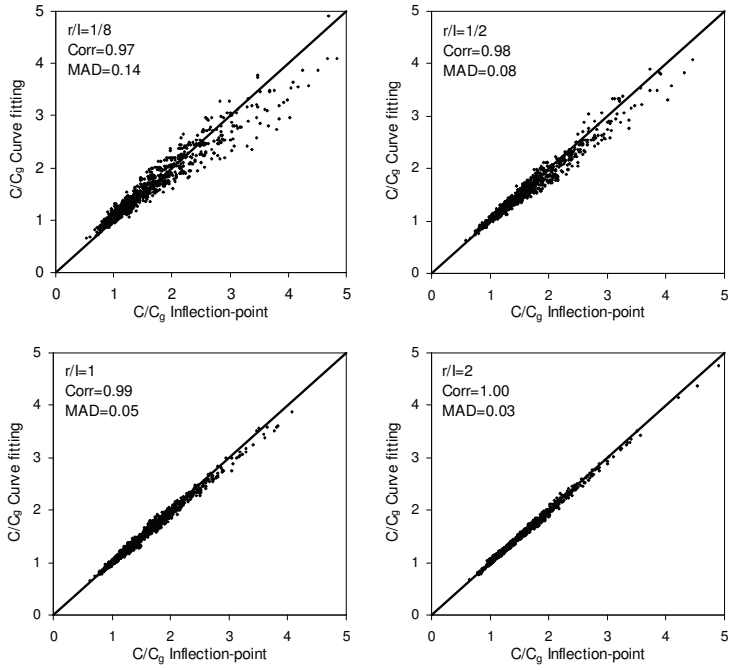

Figure 5.13: Normalized aquitard conductance estimated using the inflection-point and the curve fitting methods for different distances from the pumping well (uniform aquifer with $T_o = 1m^2/day$, and spatially variable aquitard with $C_g = 0.01day^{-1}$, $I = 8m$, and $\sigma^2 = 1$).

5.4 Conclusions

This paper examines the impact of heterogeneity of leaky aquifer systems on the flow parameters estimated with three different methods, two of them commonly used in real applications: the inflection-point [42], the curve fitting [99] methods, plus the recently developed double inflection-point method [93].

We simulate two framework scenarios whereby the aquifer or aquitard are assumed homogeneous, while the other is defined as a multiGaussian SRF with given geostatistical parameters. For the case of spatially variable transmissivity and uniform aquitard conductance, the following observations can be made:

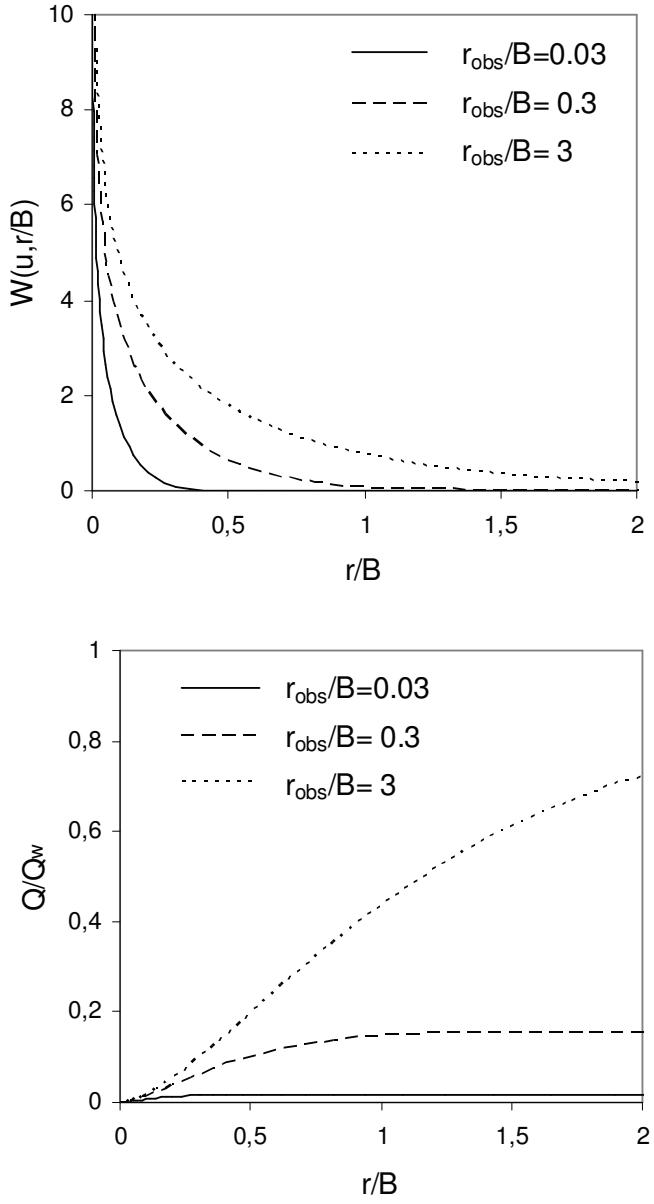

Figure 5.14: Leaky well function and vertical flow through the aquitard as a fraction of the pumping rate vs. r/B at the inflection point $t_p = r_{obs}SB/2T$ for different values of r_{obs}/B.

1. For observation points located relatively far from the well, all interpretation methods yield similar estimates of the transmissivity, storativity and aquitard conductance.

2. The expected value of the transmissivity estimates depend on the geostatistical parameters of the T field, on the leakage factor, and the distance to the pumping well. For the Hantush inflection method and the Walton method the estimates are slightly larger than the geometric mean of the point T values.

3. The T estimates from the individual realization are dependent on the location of the observation point relative to the pumping well, in contrast to the case of confined aquifers where the estimated T is relatively insensitive to the observation well location and tends to be close to the geometric mean.

4. A slight increasing trend is observed in the expected value of the estimated leakage factor and transmissivity with distance from the pumping well.

5. Because the two DIP estimates rely on different portions of the time drawdown data, they may differ from each other. The geometric mean of the two DIP estimates is generally in good agreement with the estimate obtained from the inflection-point method, particularly for distances greater than the integral scale of T. Moreover, differences in the estimates of T obtained with the inflection-point and DIP methods are correlated with the local value of T at the pumping well. This correlation tends to decrease with distance from the pumping well. Therefore, using the drawdown data at an observation point, located close to the well ($r < I$), it is possible to infer local contrasts in the transmissivity.

The second scenario assumes a uniform aquifer transmissivity and a heterogeneous aquitard. Based on the results of these simulations we conclude:

6. The heterogeneity of the aquifer and aquitard influence the estimated hydraulic parameters in distinct manners. For the case of spatially variable aquitard, the agreement in the trans-

missivity and storativity estimates obtained with the inflection-point and the curve fitting methods is very good near the pumping well. The estimation of the aquitard conductance shows an opposite trend. With increasing distance, both T and S estimates exhibit larger variability.

7. The expected value of the aquitard conductance is close to the arithmetic mean of the C values, indicating that the drawdown is most sensitive to the local conductance at the pumping well, with the sensitivity rapidly decreasing with distance.

Overall, this numerical exercise provides a framework to understand the implications of the assumption of homogeneity in the estimates obtained with the different methods commonly used in the interpretation of pumping tests in aquifer-aquitard systems. Since each method give different emphasis to different portions of the drawdown curve and, consequently to different volumes of the aquifer-aquitard system, we conclude that using all analysis methods jointly may provide additional information (specifically, about contrasts in the local value of the transmissivty at the pumping well) than using each method independently.